Journal of Bacteriology

Impact of a Transposon Insertion in *phzF2* on the Specialized Metabolite Production and Interkingdom Interactions of Pseudomonas aeruginosa

Vanessa V. Phelan, Wilna J. Moree, Julieta Aguilar, Dale S. Cornett, Alexandra Koumoutsi, Suzanne M. Noble, Kit Pogliano, Carlos A. Guerrero and Pieter C. Dorrestein

J. Bacteriol. **2014, 196(9):1683. DOI: 10.1128/JB.01258-13. Published Ahead of Print 14 February 2014.**

JB
Journals.ASM.org

Impact of a Transposon Insertion in *phzF2* on the Specialized Metabolite Production and Interkingdom Interactions of *Pseudomonas aeruginosa*

Vanessa V. Phelan,[a] Wilna J. Moree,[a] Julieta Aguilar,[b] Dale S. Cornett,[c] Alexandra Koumoutsi,[d]* Suzanne M. Noble,[d] Kit Pogliano,[b] Carlos A. Guerrero,[e] Pieter C. Dorrestein[a,e,f]

Skaggs School of Pharmacy and Pharmaceutical Sciences, University of California at San Diego, La Jolla, California, USA[a]; Division of Biological Sciences, University of California at San Diego, La Jolla, California, USA[b]; Bruker Daltonics, Billerica, Massachusetts, USA[c]; Microbiology and Immunology Department, University of California at San Francisco, San Francisco, California, USA[d]; Department of Chemistry and Biochemistry, University of California at San Diego, La Jolla, California, USA[e]; Department of Pharmacology, University of California at San Diego, La Jolla, California, USA[f]

In microbiology, gene disruption and subsequent experiments often center on phenotypic changes caused by one class of specialized metabolites (quorum sensors, virulence factors, or natural products), disregarding global downstream metabolic effects. With the recent development of mass spectrometry-based methods and technologies for microbial metabolomics investigations, it is now possible to visualize global production of diverse classes of microbial specialized metabolites simultaneously. Using imaging mass spectrometry (IMS) applied to the analysis of microbiology experiments, we can observe the effects of mutations, knockouts, insertions, and complementation on the interactive metabolome. In this study, a combination of IMS and liquid chromatography-tandem mass spectrometry (LC-MS/MS) was used to visualize the impact on specialized metabolite production of a transposon insertion into a *Pseudomonas aeruginosa* phenazine biosynthetic gene, *phzF2*. The disruption of phenazine biosynthesis led to broad changes in specialized metabolite production, including loss of pyoverdine production. This shift in specialized metabolite production significantly alters the metabolic outcome of an interaction with *Aspergillus fumigatus* by influencing triacetylfusarinine production.

In patients with cystic fibrosis (CF), mutations within the CF transmembrane conductance regulator (CFTR) lead to decreased mucociliary clearance and accumulation of thick and sticky bronchial mucus, providing a nutrient-rich environment for opportunistic pathogens to flourish (1, 2). These chronic biofilm-based infections lead to respiratory failure, the need for lung transplantation, or untimely death. When describing chronic microbial infections in CF, discussion usually revolves around a single microorganism and its interaction with the immune system. However, the human respiratory tract contains a dynamic microbial community, with a decline in lung function of CF patients correlating to a decrease in microbial diversity (3, 4). While modern sequencing techniques allow us to peer into the complexity of these microbial communities, little is known about how these microbes interact and compete on a molecular level.

Two opportunistic pathogens affecting CF patients are the Gram-negative bacterium *Pseudomonas aeruginosa* and the filamentous fungus *Aspergillus fumigatus*. In a recent clinical retrospective, coinfection with *P. aeruginosa* and *A. fumigatus* correlated with a significant decrease in lung function relative to that seen with diagnosis of *P. aeruginosa* or *A. fumigatus* infection alone (5). Concurrent detection of *P. aeruginosa* and *A. fumigatus*, using both traditional culturing techniques and modern sequencing methods, indicates that these two organisms may interact within the CF lung (3, 5–7). One way these organisms interact is through the production and secretion of small-molecule effectors called specialized metabolites, including quorum sensors, virulence factors, and natural products (previously referred to as secondary metabolites) (8, 9). *In vitro* studies show that metabolites secreted by *P. aeruginosa* inhibit *A. fumigatus* filamentation and biofilm formation (10). In 2012, we detailed the metabolic interaction between these two microbes, with an emphasis on the *A. fumigatus* Af293-mediated biotransformation of the phenazine class of specialized metabolites produced by *P. aeruginosa* PA14 (11). The phenazines have a number of roles in both intra- and interspecies interactions, including antibacterial and antifungal activities, electron shuttling through their redox capabilities, generation of reactive oxidative species, and cell signaling (12, 13). Due to the myriad of roles for the phenazine molecular family, we hypothesized that hampering the biosynthetic capacity of *P. aeruginosa* to produce the phenazines would alter the exchange of specialized metabolites between it and *A. fumigatus*.

P. aeruginosa utilizes two biosynthetic gene clusters (*phz1* and *phz2*; 98% identity) to produce five characterized phenazines: 1-hydroxyphenazine (1-HP), pyocyanin (PYO), phenazine-1-carboxylic acid (PCA), phenazine-1-carboxamide (PCN), and 5-methyl phenazine-1-carboxylic acid (5-MPCA) (14). Phenazine biosynthesis begins with the shikimate pathway and diverges into dedicated phenazine biosynthesis through the enzymatic activity of PhzF (Fig. 1). PhzF is proposed to catalyze the isomerization of *trans*-2,3-dihydro-3-hydroxyanthranilic acid (DHHA) to 6-amino-5-oxocyclohex-2-ene-1-carboxylic acid (15, 16). Subse-

Received 24 October 2013 Accepted 11 February 2014
Published ahead of print 14 February 2014
Address correspondence to Pieter C. Dorrestein, pdorrestein@ucsd.edu.
* Present address: Alexandra Koumoutsi, Genome Biology Research Unit, European Molecular Biology Laboratory, Heidelberg, Germany.
Supplemental material for this article may be found at http://dx.doi.org/10.1128/JB.01258-13.

doi:10.1128/JB.01258-13

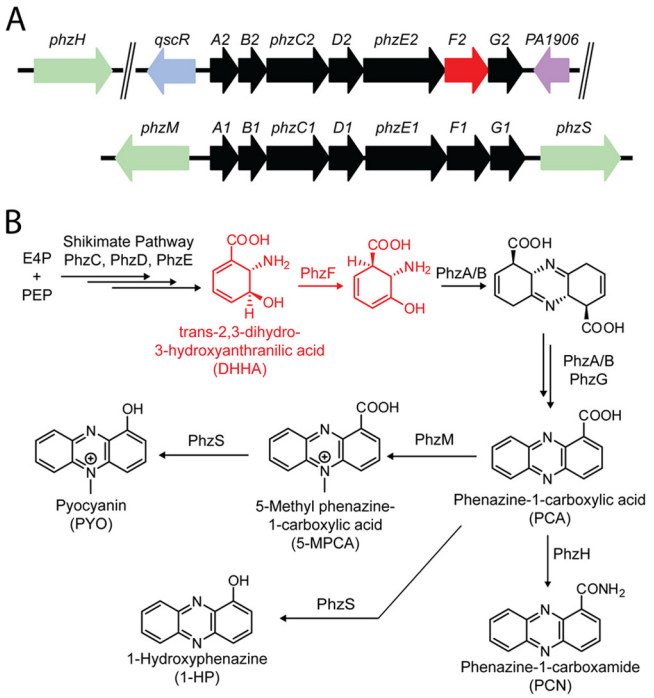

FIG 1 (A) The phenazine molecular family is biosynthesized over two core gene clusters, *phz1* and *phz2* (black; *phzA1-G1* and *phzA2-G2*) and three accessory genes (green; *phzS*, *phzM*, and *phzH*). The *phz2* cluster also contains a regulator *qscR* (blue). PA1906 (purple) is not involved in phenazine biosynthesis. The *phz2* gene cluster is hypothesized to be responsible for total phenazine biosynthesis in colony biofilms. *phzF2* (red) is the position of transposon insertion used for these studies. (B) Proposed biosynthetic schematic of the phenazines by *P. aeruginosa*. PhzF is proposed to catalyze the isomerization of DHHA (red). This step is the first dedicated step in phenazine production and is disrupted by the transposon insertion. E4P, erythrose-4-phosphate; PEP, phosphoenolpyruvate.

quent dimerization by PhzA/B and poorly defined oxidation lead to the production of PCA (17). Additional reduction, methylation, and amidation result in the formation of 1-HP, PYO, PCN, and 5-MPCA (14). Recent results suggest that although both *phz1* and *phz2* phenazine biosynthetic cassettes are capable of producing PCA, the *phz2* cluster is sufficient for phenazine production in colony biofilms (18, 19).

Herein, we describe the utility of agar-based microbial matrix-assisted laser desorption ionization (MALDI) imaging mass spectrometry (IMS) to investigate the role of the *phzF2* gene in the metabolic discussion between *P. aeruginosa* PAO1 and *A. fumigatus* Af293 in a side-by-side interaction. In this study, we utilized a transposon insertion mutant of the *phzF2* gene to highlight the chemotypic differences between the *phzF2* mutant and wild-type PAO1 despite their similar phenotypic interactions with Af293. Using a combination of qualitative (IMS) and semiquantitative (liquid chromatography-tandem mass spectrometry [LC-MS/MS]) mass spectrometry-based analyses, we confirmed the role of the *phz2* gene cluster in phenazine production of colony biofilms, showing that disruption of homeostatic phenazine production results in drastic changes in the production of other molecular families by *P. aeruginosa* and leads to altered production of *A. fumigatus* siderophore virulence factors which can be modulated by the addition of single phenazines. Taken together, these results show how modern mass spectrometry techniques can be used with traditional molecular biology to provide new insights into global specialized metabolite production, extending our knowledge of the complicated network of *P. aeruginosa* effector molecules and their roles in both intra- and interspecies interactions.

MATERIALS AND METHODS

General. *Aspergillus fumigatus* Af293 was a gift from the J. Craig Venter Institute (Nierman lab, Rockville, MD). *Pseudomonas aeruginosa* PAO1 and the *phzF2* mutant (PW4336; genotype, PA1904-G08:ISlacZ/hah) were acquired from the University of Washington's Seattle *P. aeruginosa* PAO1 transposon mutant library (20). All chemicals used for preparation of ISP2 media were purchased from Sigma-Aldrich. Organic solvents for extraction and LC-MS/MS were purchased from J. T. Baker. Universal MALDI matrix was purchased from Sigma-Aldrich. 1-Hydroxyphenazine (1-HP) (≥95% by gas chromatography [GC]) was purchased from TCI. Pyocyanin (PYO) (≥98% by high-performance liquid chromatography [HPLC]), 2-heptyl-3-hydroxy-4(1H)-quinolone (PQS) (≥96% by HPLC), and 3-oxo-C_{12}-homoserine lactone (C_{12}-HSL) were purchased from Sigma-Aldrich. Phenazine-1-carboxamide (PCN) (95% by nuclear magnetic resonance [NMR]) and phenazine-1-carboxylic acid (PCA) (95% by NMR) were purchased from Princeton Biomolecular Research, Inc. 1-HP, PCN, and PCA were purified by HPLC as previously described, as they contained multiple phenazines (11). ^{1}H NMR multiplicities are abbreviated as follows: s, singlet; d, doublet; t, triplet; q, quartet; b, broad; and a, apparent; combinations thereof are indicated.

Confirmation of transposition insertion location. Since the two phenazine biosynthetic gene clusters in *P. aeruginosa* are 98% identical, the position of the transposon insertion in the *phzF2* gene was confirmed by PCR. PAO1 was streaked onto Luria broth (LB) agar from glycerol stock. As the transposon insertion carries a tetracycline resistance cassette, the *phzF2* mutant was streaked onto LB agar containing 60 μg/ml of tetracycline from glycerol stock. After 24 h of incubation at 30°C, single colonies of PAO1 were subcultured into 2 ml of liquid LB media and single colonies of the *phzF2* mutant were subcultured into 2 ml of liquid LB media containing 60 μg/ml of tetracycline. Genomic DNA was isolated using the Promega Wizard genomic DNA purification kit. Considering the high sequence identity between the *phz1* and *phz2* biosynthetic clusters and the location of the *phzF1* and *phzF2* genes within the biosynthetic clusters, a common forward primer complementing *phzE1* and *phzE2* (5′-CGGTCCCTACCTCAAGAAGA-3′) and divergent reverse primers were used. For the *phz1* cluster, a reverse primer complementing the sequence of *phzS* was designed (5′-CGGTCTACCATCGGGTACTG-3′). The gene *phzS* immediately follows the *phzG1* gene and does not have a homolog in the *phz2* cluster. For the *phz2* cluster, a reverse primer complementing the sequence of *PA1906* was designed (5′-GTCCAACCCCG AACATCGTC-3′). PA1906 is a protein of unknown function, and the *PA1906* gene immediately follows the *phzG2* gene and does not have a homolog in the *phz1* cluster. Agarose gel electrophoresis of PCR products confirmed the transposon location in the *phzF2* gene (see Fig. S1 in the supplemental material).

Synthesis of 5-methyl phenazine-1-carboxylic acid (5-MPCA). (i) Benzyl 1-phenazinecarboxylate. Phenazine 1-carboxylic acid (45.0 mg, 201 μmol, 1.00 eq) and K_2CO_3 (55.5 mg, 402 μmol, 2.00 eq) were combined in a 4-ml glass vial containing a stir bar. This was sealed with a septum screw cap and evacuated using high vacuum (<1 torr) by piercing the septum with a needle connected to the vacuum source. The vessel was then refilled with argon, and anhydrous dimethylformamide (DMF) was added via syringe (2.00 ml, furnishing a 0.1 M solution neglecting the volume of reactants and reagents). This furnished a thick suspension. Benzyl chloride (BnCl; 35.0 μl, 302 μmol, 1.50 eq) was added using a microliter syringe. The reaction vessel was then immersed in an oil bath preheated to 80°C and maintained there with magnetic stirring for approximately 12 h. After this time, the reaction vessel was removed from the heating bath and allowed to cool to ambient temperature. A fine, colorless solid was observed at the bottom of the reaction mixture (likely

KCl); otherwise a golden yellow-brown solution was obtained. This mixture was transferred to a separatory funnel, rinsing the reaction vessel with copious amounts of diethyl ether (20 to 25 ml). The organic portion was washed five times successively with approximately 2 ml of H_2O. Then the organic portion was washed with saturated aqueous NaCl (5 ml) and subsequently dried over anhydrous Na_2SO_4, filtered, and concentrated by rotary evaporation. The material was deemed sufficiently pure to be carried forward without further purification (see characterization data and spectra). A total of 63.0 mg (>99%) of crude material was isolated as a golden yellow oil of ≥95% purity. ^{1}H NMR (500 MHz, $CDCl_3$) δ 8.39 (dd, J = 8.39, 1.70 Hz, 1 H), 8.34 to 8.29 (m, 1 H), 8.27 (dd, J = 6.85, 1.15 Hz, 1 H), 8.26 to 8.22 (m, 1 H), 7.89 (at, J = 3.45 Hz, 1 H), 7.87 (at, J = 3.40 Hz, 1 H), 7.85 (dd, J = 8.60, 6.90 Hz, 1 H), 7.62 (d, J = 6.85 Hz, 2 H), 7.43 (at, J = 6.90 Hz, 2 H), 7.37 (at, J = 7.45 Hz, 1 H), 5.59 (s, 2 H). ^{13}C NMR (125 MHz, $CDCl_3$) δ 165.44, 142.63, 142.11, 141.52, 139.98, 134.79, 132.31, 131.12, 130.27, 130.17, 129.91, 129.20, 128.32, 128.03, 127.48, 127.18 (2 C), 66.27. High-resolution mass spectrometry (HRMS) observed, 315.1133; calculated, 315.1128; error, 1.6 ppm.

(ii) Benzyl 5-methylphenazinium-1-carboxylate. To a solution of benzyl 1-phenazinecarboxylate (63.0 mg, 200 μmol, 1.00 eq) in anhydrous CH_2Cl_2 (2.00 ml) under argon was added methyl trifluoromethanesulfonate (see below; freshly prepared, 68.0 μl, 601 μmol, 3.00 eq) via microliter syringe. The reaction mixture was stirred magnetically at ambient temperature and was a solution at the start of the reaction, but after approximately 12 h, it had become an avocado green suspension. After this time interval, the reaction mixture was merely evaporated to dryness on a rotary evaporator (gradually achieving a maximum vacuum of ~10 torr) followed by high vacuum (<1 torr). The residue was used without further purification for ester hydrolysis. HRMS observed, 329.1294; calculated, 329.1285; error, 2.7 ppm. (Methyl trifluoromethanesulfonate was freshly prepared as previously described by injecting dimethyl sulfate [2.00 ml] into trifluoromethanesulfonic acid [1.45 ml] in a flask under argon that had previously been flame dried and equipped with a stir bar [21]. The mixture was stirred magnetically for 1 h at ambient temperature, after which the plastic cap used to seal the reaction was removed and replaced with a short-path distillation head. A distillation was conducted at ambient pressure, with methyl trifluoromethanesulfonate distilling at approximately 100°C. It should be noted that methyl trifluoromethanesulfonate is a strong alkylating agent and should be generated and handled only by a trained chemist.)

(iii)5-MPCA. Benzyl 5-methylphenazinium-1-carboxylate (1.0 mg, 3 μmol) in acetonitrile (100 μl) and *Pseudomonas fluorescens* esterase (1.0 mg; Sigma-Alrich) in Tris buffer (pH 7.5, 500 μl) were combined in a 1.5-ml Eppendorf tube. The reaction mixture was incubated for 3 h at room temperature. 5-Methyl phenazine-1-carboxylic acid (5-MPCA) was purified from the crude mixture using an Agilent Technologies 1260 HPLC with a diode array detector. Samples were introduced manually using a 300-μl injection volume on to a Phenomenex Luna 4-μm Synergi Polar-RP column (10.0 mm by 250 mm). The crude mixture was fractionated (35 fractions, 5 ml each) using a linear water-acetonitrile gradient (from 95:5 to 5:95 water/acetonitrile) containing 0.1% formic acid with a flow rate of 5 ml/min. A 1-μl volume of each fraction was mixed 1:1 with a saturated solution of universal MALDI matrix in 78% acetonitrile containing 0.1% formic acid and spotted onto a Bruker MSP 96 anchor plate. The sample was dried and subjected to matrix-assisted laser desorption ionization–time of flight mass (MALDI-TOF) analysis by either a Bruker Daltonics Autoflex Speed or Microflex. Mass spectra were obtained as a single spot acquisition of 100 shots. MALDI-TOF MS data were analyzed by FlexAnalysis 3.0 software. Fractions with an *m/z* corresponding to 5-MPCA were combined and lyophilized. 5-MPCA was isolated as a yellow powder (400 μg, 58% yield). HRMS observed, 239.0816; calculated, 239.0815; error, 0.4 ppm.

Genetic complementation of the *phzF2* mutant. Plasmid pJA09 (pP_{ara}phzF2) was constructed from PCR amplification of *phzF2* from genomic DNA of *P. aeruginosa* PAO1 using oligonucleotides 5′-TAAAA CGACGGCCAGTGCCAAGCTTTCACAGGTAGGCGCGGCCTTCGG CG-3′ and 5′-TACCCATGGGATCTGATAAGAATTCAAGGAGGATTT TAGAATGCACAGATATGTCGTGATAG-3′ with a ribosome binding site (AAGGAGGA) 7 bp upstream of the start site of *phzF2*; PCR amplification of pHERD30T (22) using oligonucleotides 5′-GAATTCTTATCA GATCCCAT-3′ and 5′-AAGCTTGGCACTGGCCGTCG-3′ and Gibson Assembly (New England BioLabs) was used to join *phzF2* and pHERD30T. The constructed plasmid was transformed into chemically competent *Escherichia coli* strain TOPO10 and selected on gentamicin plates. Construction was confirmed by sequencing performed by Genewiz. Plasmid pJA09 was then introduced into electrocompetent PAO1 *phzF2* mutant cells by electroporation with Gene Pulser Xcell (Bio-Rad) using *P. aeruginosa* settings and selected on LB agar plates containing 25 μg/ml of gentamicin.

Culture of colony biofilms and interactions. PAO1, the *phzF2* mutant, and the complemented PhzF2 pJA09-bearing strain were grown from a single colony in LB media overnight to stationary phase (optical density [OD] = 1.2), diluted to a 1.6×10^8-CFU/ml, 20% glycerol stock, and stored at −80°C in 50-μl aliquots. Af293 spore stock was prepared as previously described (7.2×10^6-CFU/ml, 20% glycerol stock) and stored at −80°C in 50-μl aliquots (11). These frozen stocks were used directly for inoculations.

P. aeruginosa (1.6×10^6 CFU; PAO1 or the *phzF2* mutant) was inoculated at a 5-mm distance from an inoculant of Af293 (7.2×10^4 CFU) on 10 ml of ISP2 agar (1% malt extract, 0.4% yeast extract, 0.4% glucose, and 2% agar) in 100- (outside diameter) by 25-mm petri dishes (Fisherbrand). The cultures were incubated for 48 h at 30°C. For chemical complementation, corresponding compounds were spotted directly onto the growth medium at a final amount of 40 nmol. The organic solution was allowed to dry, and the *P. aeruginosa* strains were inoculated directly on top of the chemical complement, with Af293 inoculated 5 mm away. *P. aeruginosa* (PAO1, the *phzF2* mutant, or the complemented PhzF2 pJA09-bearing strain) and Af293 controls were inoculated similarly, including those for chemical complementation. For genetic complementation, the PhzF2 pJA09-bearing strain was induced on ISP2 agar containing 0.2% L-arabinose.

MALDI-IMS. For IMS experiments, a region of agar including the colony biofilm or interaction was excised and laid upon a Bruker Daltonics MALDI MSP 96 anchor target plate. A photograph was taken of the MALDI target holding the agar samples. Af293 aerial hyphae were removed from the surface of the colony using a cotton swab dampened with acetonitrile. Universal MALDI matrix (Sigma-Aldrich) was applied using a 53-μm sieve, and samples were dried at 37°C for a minimum of 6 h. All colonies were subjected to MALDI-TOF MS in positive reflectron mode using a 400- to 600-μm spatial resolution in XY by either a Bruker Daltonics Autoflex Speed or Microflex. The data from both instruments were analyzed using FlexImaging 3.0. Detailed parameters for microbial IMS have been published elsewhere (11, 23–26). For high-resolution MALDI IMS, a duplicate 48-h culture was subjected to IMS on a 9.4T solariX Fourier transform-ion cyclotron resonance (FT-ICR) mass spectrometer equipped with a dual electrospray ionization (ESI)/MALDI ion source and Smartbeam II laser set to minimum focus. The *m/z* range acquired was 175 to 375, with a transient length of 700 ms for a broadband resolving power of approximately 150,000. Single-point calibration was used utilizing the dihydroxybenzoic acid (DHB) cluster ion at *m/z* 273.03936 as lock mass. Data were acquired with a 200-μm spatial resolution.

Extraction procedure. For general chemical extraction, the agar of entire single plates including the colony biofilms was sliced into small pieces and extracted with 10 ml of ethyl acetate followed by 10 ml of methanol. The solvent was separated from agar pieces by filtration and concentrated *in vacuo*. Combined ethyl acetate-methanol extracts were resuspended in 1 ml of methanol and centrifuged prior to analysis.

LC-MS/MS analysis. For LC-MS/MS analysis, samples were diluted 10-fold. Mass spectrometry was performed by using a Bruker Daltonics Maxis qTOF mass spectrometer equipped with a standard electrospray

ionization source. The mass spectrometer was tuned by infusion of Tuning Mix ES-TOF (Agilent Technologies) at a 3-μl/min flow rate. For accurate mass measurements, lock mass internal calibration used a wick saturated with hexakis(1H,1H,3H-tetrafluoropropoxy)phosphazene ions (Synquest Laboratories; *m/z* 922.0098) located within the source. Samples were introduced by a Thermo Scientific UltraMate 3000 Dionex ultraperformance liquid chromatograph (UPLC) using a 20-μl injection volume. Ethyl acetate-methanol extracts were separated using a Phenomenex Luna 5-μm C_{18}(2) column (2.0 mm by 250 mm). A linear water-acetonitrile gradient (from 98:2 to 2:98 water/acetonitrile) containing 0.1% formic acid was utilized. The flow rate was 0.2 ml/min. The mass spectrometer was operated in data-dependent positive-ion mode, automatically switching between full-scan MS and MS/MS acquisitions. Full-scan MS spectra (*m/z* 50 to 2,000) were acquired in the TOF, and the top 10 most intense ions in a particular scan were fragmented using collision-induced dissociation at 35 eV for +1 ions and 25 eV for +2 ions in the collision cell. Structural verification of ions identified by full-scan MS in IMS was performed manually by comparing the exact mass for the full scan and the MS/MS spectra with previously reported structural characterization (11).

Data analysis. IMS data analysis was performed using Bruker Daltronics FlexImaging v3.0. Visualization of ion intensity was optimized to highlight differences between samples being compared. Ions identified by full-scan MS in low-resolution IMS were structurally verified by matching the distribution and nominal mass to the exact mass measured by high-resolution (HR) IMS. These metabolites were further characterized by LC-MS/MS. LC-MS/MS data analysis was performed using Bruker Daltronics DataAnalysis v4.1 (Build 362.7). Lock mass internal calibration using hexakis(1H,1H,3H-tetrafluoropropoxy)phosphazene ions (Synquest Laboratories; *m/z* 922.0098) was applied. Extracted ion chromatograms (EICs) using the exact mass of a metabolite of interest were created. The MS/MS spectra from these EICs were manually compared with previously reported data (11). To calculate fold changes, the areas of EICs were calculated for three independent cultures, averaged, and compared between cultures of interest.

RESULTS AND DISCUSSION

Interaction of *P. aeruginosa phzF2* mutant and *A. fumigatus*. Transposon mutants have been an invaluable tool for connecting genotypes to phenotypes. They have been used to identify key genes in *P. aeruginosa* signaling pathways. Considering that the phenazine molecular family produced by *P. aeruginosa* has been identified as key participants in both intra- and interspecies interactions, we hypothesized that disrupting phenazine biosynthesis would result in an altered metabolic response by *A. fumigatus* Af293. While the *P. aeruginosa* genome contains two biosynthetic gene clusters for phenazine biosynthesis, *phz1* and *phz2*, the *phz2* gene cluster has been shown to be sufficient for wild-type phenazine production in *P. aeruginosa* PA14 colony biofilms (7, 14, 19). To test whether this observation held true for PAO1, we chose to use a publicly available transposon insertion mutant of the *phzF2* gene in the *phz2* gene cluster. PhzF is the first dedicated step in phenazine biosynthesis, and disruption of the *phzF2* gene should be sufficient to prevent phenazine biosynthesis in colony biofilms (15–17).

To reveal the outcome of altered phenazine production, the *phzF2* mutant and Af293 were inoculated side by side. Concurrently, a wild-type PAO1-Af923 interaction was prepared similarly in separate culture. The colony biofilms of PAO1 and the *phzF2* mutant were phenotypically similar and showed comparable degrees of inhibition of Af293. Both samples were subjected to microbial IMS. It is important to note that in order to compare relative signal intensity between two samples, the microbial IMS data must be acquired from a single MALDI plate in a single experiment. While the molecular distributions visualized in IMS can be compared between experiments, the intensity of those molecular features cannot.

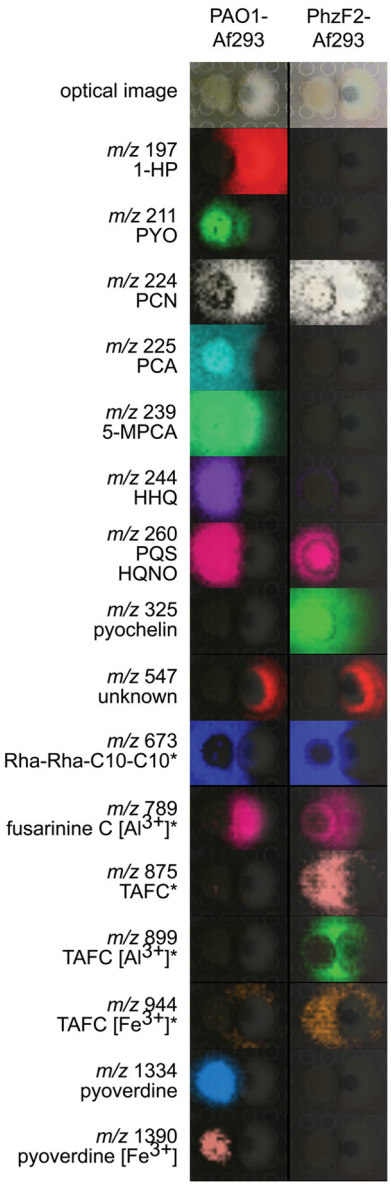

FIG 2 Microbial IMS images of selected metabolites produced by *P. aeruginosa* (left microbial colony) and *A. fumigatus* (right microbial colony) grown on ISP2 media for 48 h. Optical images are displayed in the top row. Both *P. aeruginosa* PAO1 and the *phzF2* mutant are capable of inhibiting *A. fumigatus* Af293. All other images are overlays of falsely colored *m/z* distributions over optical images. The interaction of PAO1 and Af293 yielded metabolite production similar to that previously reported, including localization of 1-HP under the Af293 colony (11). The *phzF2* mutant interaction with Af293 resulted in strikingly different metabolite production. Phenazine production was reduced, with the exception of PCN, which was produced in larger amounts. Both quinolone and pyoverdine production were also reduced. Rhamnolipid and pyochelin production was increased. In response, TAFC production by Af293 was increased. An asterisk denotes sodium salt.

Strikingly, the *phzF2* mutant interaction with Af293 had stark differences in specialized metabolite production compared to the PAO1-Af293 wild-type interaction (Fig. 2; see also Fig. S2 and

Table S1 in the supplemental material). As expected, changes in phenazine production were observed. However, unlike in previous reports indicating that the *phz2* gene cluster was responsible for total phenazine biosynthesis in PA14 colony biofilms, the transposon insertion in the *phzF2* gene of PAO1 resulted in decreased production of 1-HP, PYO, PCA, and 5-MPCA but in increased production of PCN (19). Surprisingly, production of other *P. aeruginosa* molecular families was also affected, including downregulation of the quinolones and upregulation of the rhamnolipids. The most marked change in specialized metabolite production for both *P. aeruginosa* and *A. fumigatus* was the difference in siderophore production between the PAO1 and *phzF2* mutant interactions. In aerobic environments, iron exists as ferric (Fe^{3+}) oxides and is not bioavailable, while in human hosts, iron is bound to transport and storage proteins. In order to acquire iron from the environment, microbes produce small molecules with high iron affinity called siderophores (27). For many pathogens, including *P. aeruginosa* and *A. fumigatus*, siderophores have been shown to be important for virulence and capable of sequestering iron from host proteins (28–30). *P. aeruginosa* and *A. fumigatus* each have the biosynthetic capacity to produce two extracellular siderophores (29, 31, 32). *P. aeruginosa* produces pyochelin and pyoverdine, while *A. fumigatus* produces fusarinine C and triacetylfusarinine C (TAFC). In the *phzF2* mutant interaction with Af293, we observed reduced pyoverdine production and increased pyochelin production by the *phzF2* mutant and increased TAFC production by Af293 compared to the wild-type interaction.

Effect of disrupting *phzF2* on *P. aeruginosa* specialized metabolite production. Due to the clear differences in *P. aeruginosa* specialized metabolite production between the PAO1 and *phzF2* mutant interactions with Af293, we hypothesized that the changes were foremost due to the disruption of phenazine biosynthesis. Previously, PYO had been termed a terminal signaling factor in the *P. aeruginosa* PA14 signaling cascade and implicated in the downregulation of iron acquisition genes (33). However, no published data have indicated that the phenazines play a role in maintaining the homeostatic production of the specialized metabolome of *P. aeruginosa*. In the single-species colony biofilms of PAO1 and the *phzF2* mutant, we observed the same changes in *P. aeruginosa* specialized metabolite production as in the interactions (Fig. 3). In order to quantify these changes, the entire agar plate containing a single colony biofilm was chemically extracted and subjected to liquid chromatography-tandem mass spectrometry (LC-MS/MS). Fold changes were calculated using peak area of extracted ion chromatograms (EICs) for *m/z* values corresponding to the metabolites of interest. MS/MS data from the peak in the EICs used for these calculations agree with previously published reports (11).

In regard to phenazine production, our data correspond well to previously published reports of phenazine production in knockout strains of the *phz2* gene cluster (19). Although it has been reported that a deletion of the *phz2* gene cluster resulted in complete absence of phenazine production by PA14 colony biofilms as detected by UV absorbance, we observed a 2-fold-increased production of PCN by the *phzF2* mutant compared to the PAO1 wild type. The production of PCN by the *phzF2* mutant was verified by correlating the exact mass, MS/MS fragmentation, and retention time with a commercial standard (see Fig. S3 in the supplemental material). In the *phzF2* mutant, total phenazine production was reduced to 6% compared to that by wild-type

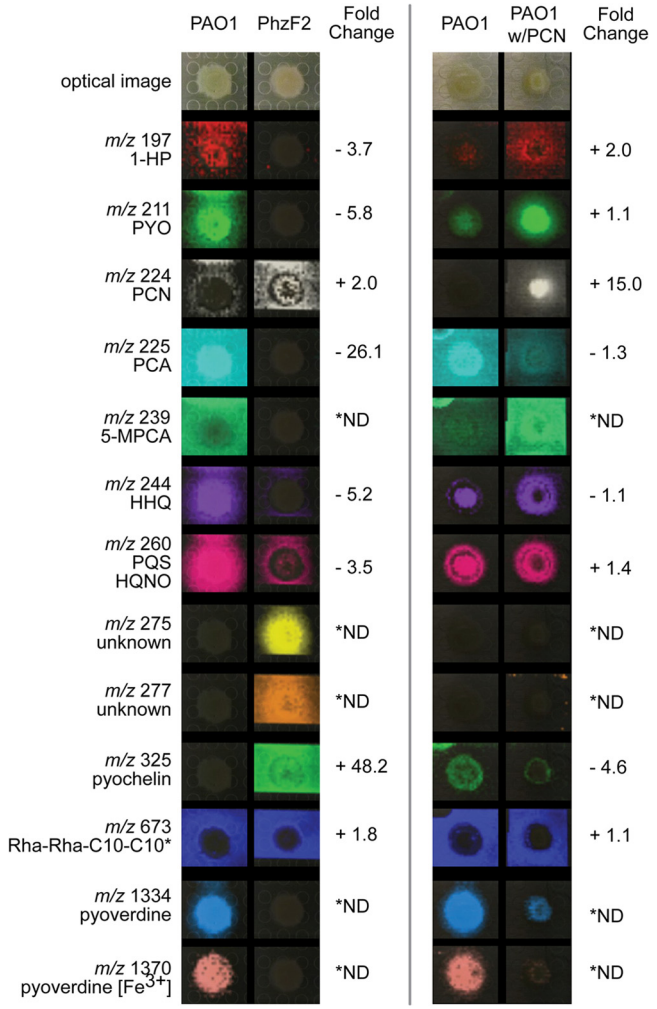

FIG 3 Microbial IMS images for selected metabolites of *P. aeruginosa* grown on ISP2. The top row displays optical images. The other images are falsely colored *m/z* distributions overlaying optical images. Fold changes were calculated based upon LC-MS/MS data. (Left) The disruption of phenazine biosynthesis in the *phzF2* transposon mutant causes production changes of specialized metabolite families. This includes decreases in phenazine (except for PCN), quinolone, and pyoverdine production. Production of the rhamnolipids and pyochelin was increased. Unknown metabolites, *m/z* 275 and 277, were produced only by the *phzF2* mutant. (Right) PCN was added to cultures of PAO1 since it was the only phenazine produced at larger amounts by the *phzF2* mutant. This led to increased production of the phenazines 1-HP, PYO, and 5-MPCA and decreased production of PCA. Both pyochelin and pyoverdine production were decreased. Neither quinolone nor rhamnolipid production was significantly affected, indicating that the change in siderophore production was independent of *rhl* and AQ signaling pathways. *ND, not detected in the extraction and subsequent LC-MS/MS analysis. An asterisk denotes sodium salt.

PAO1. PCN accounted for approximately 35% of total phenazine production in the *phzF2* mutant, compared to 1% in wild-type PAO1 (see Table S2 in the supplemental material). Reduced levels of 1-HP, PYO, and PCA were produced by the *phzF2* mutant (see Table S2 and Fig. S4 in the supplemental material). Most notably, PCA levels decreased 26-fold in the *phzF2* mutant versus the wild type, while 1-HP and PYO decreased 3.7- and 5.8-fold, respectively. The discrepancy between these results and previously published data could be due to a number of factors, including the use

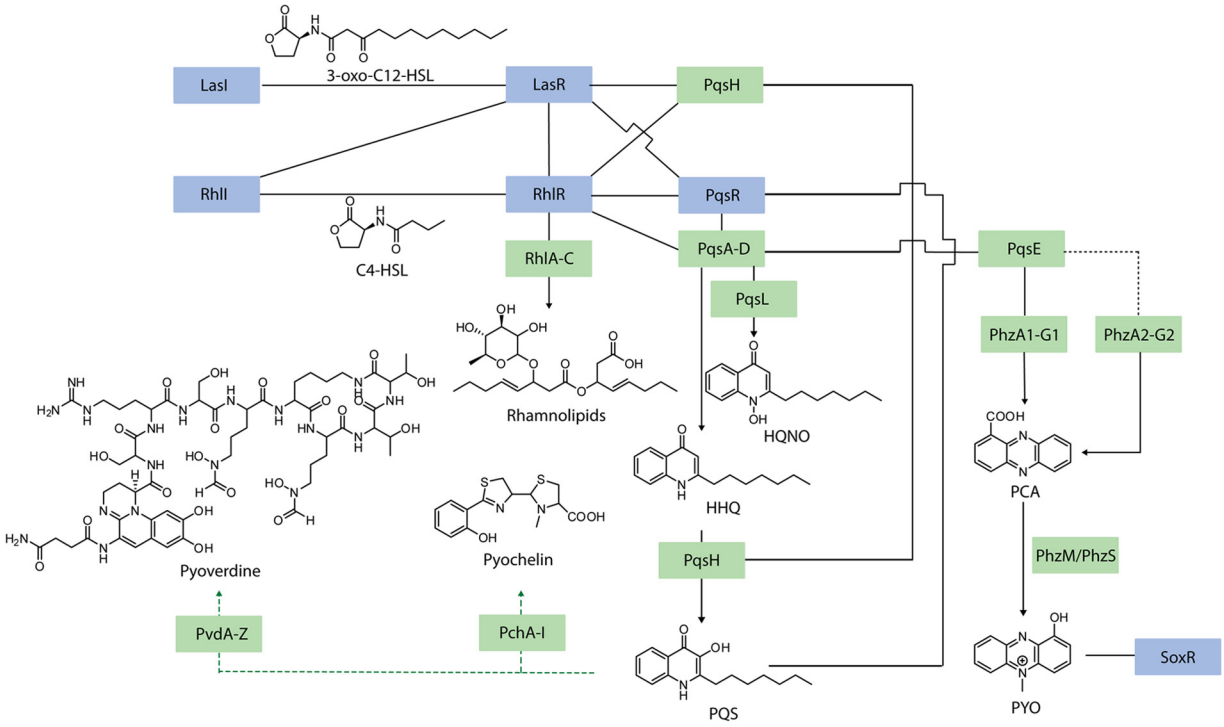

FIG 4 *P. aeruginosa* uses hierarchical signaling pathways to control specialized metabolite production. Gene regulators are represented by blue boxes, biosynthetic pathways are represented by green boxes, and structures of key metabolites are shown. The hierarchical signaling pathways of *P. aeruginosa* begin with two HSL-dependent regulatory pathways, *las* and *rhl*, linked to the AQ system. LasI produces 3-oxo-C_{12}-HSL, and RhlI produces C_4-HSL. These HSLs interact with the transcriptional regulators LasR and RhlR, respectively, to activate target promoters. The *rhl* signaling pathway directly regulates rhamnolipid biosynthesis. Both *las* and *rhl* signaling have been implicated in regulating AQ biosynthesis through the PqsR (MvfR) regulator. Of the AQ metabolites produced, only HHQ, PQS, and HQNO have defined biological activities. HHQ and PQS have been implicated in the regulation of production of the phenazine molecular family. The two best-studied phenazines are PCA and PYO. PYO has been shown to induce SoxR signaling. The link between siderophore biosynthesis and the signaling pathways remains unknown. However, PQS has been described as activating pyoverdine and pyochelin biosynthesis in a non-signaling-dependent manner.

of different strains and mutants, growth media, extraction procedures, and detection methods. These results suggest that under our growth conditions, PCN is produced by the *phz1* gene cluster (with the accessory protein PhzH), while 1-HP, PYO, PCA, and 5-MPCA are produced primarily by the *phz2* gene cluster. Interestingly, both gene clusters are known to produce PCA in PAO1. However, in this instance, the PCA produced by the *phz1* gene cluster is largely converted into PCN. From a biosynthetic standpoint, the role of the *phz2* gene cluster as the chief producer of the phenazines 1-HP, PYO, and 5-MPCA is particularly intriguing because the accessory genes required for their production (*phzS* and *phzM*) are directly upstream and downstream of the *phz1* gene cluster, respectively (14).

While changes in phenazine production of mutants within the phenazine biosynthetic pathways have been well documented, differences in production of other molecular families have never been measured directly. In *P. aeruginosa*, the most thoroughly investigated set of specialized metabolites are the homoserine lactones involved in its complex signaling network (Fig. 4). The currently proposed hierarchical signaling pathway is dependent upon two *N*-acylhomoserine lactone (HSL) regulatory circuits, *las* and *rhl*, linked to a 2-alkyl-4-quinolone (AQ) system (34). In *las*-dependent signaling, LasI produces 3-oxo-dodecanoyl-L-HSL (3-oxo-C_{12}-HSL), which interacts with the LasR transcriptional regulator, resulting in activation of target promoters (35). In addition to its signaling capabilities, 3-oxo-C_{12}-HSL has been shown to be partially responsible for inhibition of *Candida albicans* growth (36). In the *rhl* pathway, RhlI synthesizes *N*-butanoyl-L-HSL (C_4-HSL), which interacts with the RhlR transcriptional regulator, leading to the activation of target promoters (37). Both the *las*- and *rhl*-dependent signaling pathways have been implicated in the regulation of the AQ biosynthetic pathway through PqsR (also referred to as MvfR) (38). The non-HSL signaling metabolites resulting from activation of the AQ pathway are 2-heptyl-3-hydroxy-4-quinolone (*Pseudomonas* quinolone signal [PQS]) and 2-heptyl-4-quinolone (HHQ) (39–43). PQS has been shown to potentiate *las*- and *rhl*-dependent signaling, biofilm formation, and siderophore production (41). PQS and HHQ have also both been linked to the regulation of phenazine production (39).

While commercial 3-oxo-C_{12}-HSL spotted onto agar was detected using microbial IMS, endogenous HSLs were not detected under our growth conditions (see Fig. S4 in the supplemental material). Rhamnolipid production (as exemplified by Rha-Rha-C_{10}-C_{10} [*m/z* 673]) was increased 1.8-fold in the *phzF2* mutant compared to PAO1 as determined by LC-MS/MS analysis (Fig. 3; see also Table S2 and Fig. S5 in the supplemental material). The increased rhamnolipid production indicates that RhlR/RhlI-based signaling is also affected by phenazine production, since rhamnolipid biosynthesis is under the direct control of this two-

component system (44). Rhamnolipids function as biosurfactants and antifungals and are responsible for the swarming motility of *P. aeruginosa* (45). The moderate increase of rhamnolipid production in the *phzF2* mutant offers a likely explanation for the increase in colony size previously observed with phenazine knockout strains and continued inhibition of Af293 in the interaction (see Fig. S6 in the supplemental material) (46, 47).

Although *P. aeruginosa* produces a total of approximately 50 quinolones, only two signaling metabolites (HHQ and PQS) and the antibiotic 4-hydroxy-2-heptylquinoline-*N*-oxide (HQNO) have been correlated to biological activities (42, 43). Approximately 12 quinolones were detected by microbial IMS, including HHQ (*m/z* 244) and PQS/HQNO (*m/z* 260) (see Fig. S7 in the supplemental material). PQS and HQNO are structural isomers differing in the position of a hydroxyl group. Therefore, LC-MS/MS was used to differentiate between these two quinolones by their fragmentation patterns and retention times. Comparing fragmentation data to previous reported values, it was determined that the vast majority of *m/z* 260 corresponds to HQNO, not PQS (see Fig. S8 in the supplemental material) (11). The production of higher levels of HHQ than of PQS in wild-type PAO1 supports the recent hypothesis that HHQ plays a larger role in maintaining colony biofilms than PQS (19). In the *phzF2* mutant, quinolone production was reduced, with both HHQ and HQNO being produced at levels approximately 5-fold and 3.5-fold less than in PAO1, respectively (see Fig. S9 and Table S2 in the supplemental material). These results indicate that the phenazine molecular family influences the AQ signaling pathway as well.

The most prominent change between the *phzF2* mutant and PAO1 was the production of the two siderophores, pyochelin and pyoverdine (Fig. 3). PAO1 predominantly produced the siderophore pyoverdine. This is consistent with the current paradigm of iron acquisition by *P. aeruginosa* (31). Pyoverdine has higher binding affinity for iron than pyochelin, allowing it to preferentially bind iron and leading to autoinduction of the pyoverdine biosynthetic pathway. Conversely, in the *phzF2* mutant, pyochelin was the predominant siderophore produced. Quite unexpectedly, the *phzF2* mutant did not produce detectable amounts of pyoverdine, the primary siderophore of *P. aeruginosa*. One intriguing explanation for the loss of pyoverdine production is that the phenazines play a role in the reductive mechanism thought to be required for pyoverdine-dependent iron acquisition (29, 48). One of the defining characteristics of the phenazine molecular family is its redox capabilities, including the ability to reduce environmental ferric iron to ferrous (Fe^{2+}) iron (12, 49–52).

Chemical complementation of PAO1 and the *phzF2* mutant. To test whether a specific phenazine was responsible for the observed changes in siderophore production, growing cultures were directly supplemented with the phenazines 1-HP, PYO, PCA, PCN, and 5-MPCA (see Scheme S1 in the supplemental material) and subjected to IMS. Cultures of PAO1 were supplemented with PCN. PCN was the only phenazine produced at higher levels by the *phzF2* mutant. We hypothesized that PCN may play a role in siderophore production of PAO1 similar to that shown for PYO in *P. aeruginosa* PA14 exponential-phase cultures, in which exogenous PYO downregulates a contingent of iron acquisition genes, including those for pyoverdine production (33). Both siderophores pyoverdine and pyochelin were produced at decreased levels in the PCN-supplemented PAO1 cultures, again linking phenazine and siderophore production (Fig. 3; see also Table S2 in the supplemental material). It is possible that the added PCN led to reduction of Fe^{3+} to Fe^{2+}, increasing bioavailable iron and resulting in a reduced need for siderophore production. Additionally, this complementation led to increased production of the phenazines 1-HP, PYO, and 5-MPCA and reduced production of PCA (Fig. 3). Neither rhamnolipid nor quinolone production was significantly affected by the addition of PCN, indicating that the observed changes in siderophore production are independent of the *rhl* and AQ signaling pathways. Despite minor effects on total phenazine production, the addition of 1-HP, PCA, PYO, and 5-MPCA did not recover pyoverdine production of the *phzF2* mutant, although addition of PYO led to an additional 2.4-fold decrease in pyochelin production versus that of the *phzF2* mutant alone (see Fig. S10 and Table S4 in the supplemental material).

Since exogenous phenazines could not recover pyoverdine production in the *phzF2* mutant, we hypothesized that another metabolite or protein effector regulated by the signaling cascade of *P. aeruginosa* may be responsible for controlling pyoverdine production. The increased production of the rhamnolipids by the *phzF2* mutant indicated that the *rhl* signaling pathway was upregulated, making it unlikely that this signaling pathway would recover pyoverdine production. To test whether autoinducers from the *las* and AQ signaling pathways could induce pyoverdine production, cultures of the *phzF2* mutant were supplemented with 3-oxo-C_{12}-HSL to induce the *las* pathway and with PQS to induce the AQ pathway. Neither PQS nor 3-oxo-C_{12}-HSL had an effect on pyoverdine production. This indicates that other effector molecules regulated by the *las* and AQ pathways are not involved in the observed differences of siderophore production between wild-type PAO1 and the *phzF2* mutant (see Fig. S10 in the supplemental material). The inability to chemically complement the *phzF2* mutant with exogenous metabolites could be due to several possibilities. One of these possibilities is the production of an uncharacterized phenazine. Although *P. aeruginosa* is one of the most studied and characterized microbial pathogens, many of the metabolites produced remain structurally uncharacterized. Another possibility is that metabolites added exogenously are not able to correct the change in redox potential of the *phzF2* mutant. It is thought that the phenazines exist in their oxidized state in the external environment and their reduced state within the cell, creating a natural redox gradient (53). Since these experiments were carried out aerobically, the exogenous phenazines were added in their oxidized state. Although reduction of phenazines has been observed in standing cultures, it has not been empirically determined if extracellular oxidized phenazines can be transported across the cell membrane and reduced intracellularly by *P. aeruginosa* (12).

Genetic complementation of the *phzF2* mutant. Since pyoverdine production by the *phzF2* mutant could not be recovered with exogenous metabolites, we hypothesized that genetic complementation may be able to restore wild-type specialized metabolite production. To investigate this, the *phzF2* mutant was complemented in *trans* with a *phzF*-containing L-arabinose-inducible plasmid (pJA09). Only partial complementation was achieved with pJA09 (see Fig. S11 and S12 and Table S4 in the supplemental material). The pJA09 construct, without induction and therefore low levels of PhzF2, led to increased production of PYO, PCN, and the rhamnolipids, a marked decrease of pyochelin, and a moderate decrease in quinolone production compared to those of the *phzF2*

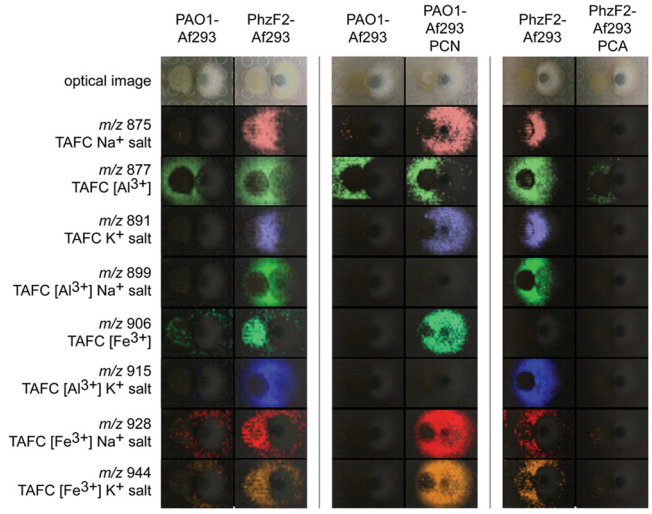

FIG 5 IMS images of the triacetylfusarinines of *A. fumigatus* Af293. The top row displays optical images. The other images are falsely colored *m/z* distributions overlaying optical images. (Left) The interaction of Af293 with the *phzF2* mutant leads to increase production of TAFC by Af293. Unbound, Al^{3+}, and low levels of Fe^{3+} forms of TAFC are detected at the interaction site. (Middle) Complementation of PAO1 with PCN results in higher production of TAFC by Af293. Only the unbound and Fe^{3+} forms of TAFC are detected throughout the fungal colony. (Right) Complementation of the *phzF2* mutant with PCA leads to decreased production of TAFC.

mutant control. Induction of the PhzF2 pJA09-bearing strain with L-arabinose led to greater production of PCA, PCN, PYO, and the rhamnolipids and larger reduction of pyochelin production, again highlighting the link between phenazine and siderophore production. Pyoverdine production was not detected in any of the samples. Although the IMS image shows increased production by the induced PhzF2 pJA09-bearing strain of *m/z* 239, corresponding to 5-MPCA, analysis of the mass spectrum reveals that this is due to the isotopic pattern of *m/z* 238, an unidentified molecule (see Fig. S13 in the supplemental material). Among the possible explanations for the partial complementation are overproduction of PhzF and polar effects of the transposon insertion in the *phzF2* gene on the downstream *phzG2*.

Effect of individual phenazines on TAFC production in *P. aeruginosa-A. fumigatus* coculture. One effect of the alteration in specialized metabolite production between the *phzF2* mutant and PAO1 was a differential response by Af293. Specifically, Af293 increased TAFC production in response to the *phzF2* mutant compared to wild-type PAO1 (Fig. 5). This was surprising, as phenazine biosynthesis is severely hindered in the *phzF2* mutant and we had previously shown that the phenazine 1-HP was able to stimulate TAFC production by *A. fumigatus* (11) In this experiment, as well as in our previous study, TAFC was detected primarily as the Al^{3+}-bound form at the interface of the interaction between *P. aeruginosa* and *A. fumigatus* (11) This highlights the dynamic nature of microbial interactions and that 1-HP is not the sole inducer of TAFC production.

PCN was the only phenazine produced at higher levels in the *phzF2* interaction than in the PAO1 interaction. While PCN cannot solely stimulate TAFC production, we hypothesized that supplementing PAO1 with PCN could influence the competition for iron between PAO1 and Af293 (11). To selectively complement PAO1, PCN was spotted onto the agar and allowed to dry. PAO1 was inoculated directly on top of the PCN and Af293 was inoculated adjacent to PAO1. Indeed, Af293 produced increased amounts of TAFC in response to PCN complemented with PAO1 (Fig. 5). Strikingly, in the interaction between Af293 and PAO1 complemented with PCN, the TAFC was predominantly detected in its unbound and Fe^{3+}-bound forms throughout the fungal colony (Fig. 5).

Since TAFC production could be induced by supplementing the PAO1 interaction with PCN, we postulated that another phenazine would be capable of turning off TAFC production in the *phzF2* mutant interaction. Therefore, the *phzF2* mutant was supplemented with 1-HP, PYO, PCA, and 5-MPCA and cocultured with Af293 (see Fig. S12 in the supplemental material). Supplementation of the *phzF2* mutant interaction with PCA led to a marked decrease in TAFC production by Af293 (Fig. 5). However, neither PYO nor 5-MPCA had any discernible effect on TAFC production, while 1-HP induced slightly higher TAFC production.

While the change in TAFC production could be attributed to the redox ability of PCA and PCN, it is unclear why these two phenazines elicit this drastic change in TAFC production while the other phenazines tested do not. 1-HP, PCA, and PCN have similar reaction rates for the reduction of ferric iron. PYO has a much lower reaction rate, providing a plausible explanation for why supplementing the *phzF2* mutant interaction with PYO had no effect on TAFC production (12, 49, 51). However, supplementation of the *phzF2* mutant interaction with 1-HP and PCA had markedly different effects on TAFC production by Af293, even though they have similar reduction potentials. This is especially surprising since Af293 can biotransform PCA to 1-HP (11). Interestingly, PCA and PCN have the opposite effect on TAFC production. PCA or PCN alone cannot induce Af293 TAFC production, highlighting a differential response between two structurally related phenazines in interkingdom interactions. Neither phenazine had any discernible effect on rhamnolipid or quinolone production by *P. aeruginosa*, indicating that the differential effect on TAFC production is not due to effector molecules controlled by the *rhl* and AQ signaling pathways of *P. aeruginosa*. These results provide the groundwork for further study of the role of phenazines in iron acquisition in interkingdom interactions.

The complexity of the microbial community within lungs of CF patients is just beginning to be appreciated. While the members of these communities are being defined by culture-independent methods, how they interact with each other is poorly understood, particularly on a molecular level (3, 54). This study used microbial IMS and LC-MS/MS in the model interaction between *P. aeruginosa* and *A. fumigatus*, two recognized pathogens of CF patients. The use of a publicly available transposon mutant early in the phenazine biosynthetic pathway revealed a link between phenazine production and iron acquisition by both *P. aeruginosa* and *A. fumigatus* (Fig. 6). While transposon mutants are traditionally used in phenotypic assays, notably, the chemotypic changes observed in both mono- and coculture occurred without affecting the visible phenotype. Considering that PCA is the most abundant phenazine produced by *P. aeruginosa* using our culture methods, readily diffuses through agar cultures, and has been detected in sputum samples, one can hypothesize that chemical through-space interactions can occur between *P. aeruginosa* and *A. fumigatus* (55). Specifically, in response to certain phenazines and their

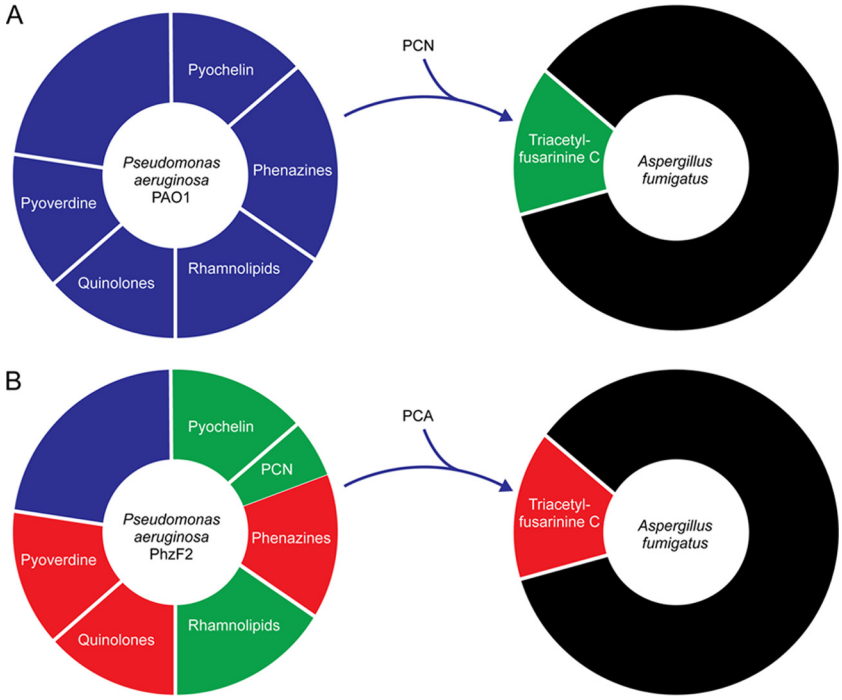

FIG 6 (A) *Pseudomonas aeruginosa* produces a number of different molecular families to interact with its environment, including neighboring microorganisms. In the interaction between *P. aeruginosa* and *A. fumigatus*, *P. aeruginosa* induces low-level production of the TAFC family. When the phenazine PCN is added to the interaction, the production levels of TAFC increase substantially. (B) A transposon insertion into a gene early in the biosynthesis of the phenazine molecular family, *phzF2*, leads to marked changes in overall specialized metabolite production. In the interaction between the *phzF2* mutant and *A. fumigatus*, TAFC production is increased. However, the addition of the phenazine PCA to the interaction is sufficient to turn off TAFC production by *A. fumigatus*. Green, increased production; red, decreased production.

inherent redox capabilities or potential roles in cell signaling, *A. fumigatus* may be able to modulate its own iron acquisition genes, including those of TAFC. It will be interesting to see how future investigations unravel the role of the phenazine class of specialized metabolites in intra- and interspecies signaling and iron acquisition.

ACKNOWLEDGMENTS

We thank Ashlee Dravis (J. Craig Venter Institute) for providing the *Aspergillus fumigatus* Af293 strain and Jane Yang for critically reviewing the manuscript. D.S.C. thanks Richard Caprioli at the Vanderbilt University Mass Spectrometry Research Center for use of the Bruker MALDI FT-ICR device.

This work was supported by National Institutes of Health grants AI095125 and S10RR029121 (P.C.D.), K01GM103809 (V.V.P.), and AI095125 (K.P.) and by the University of California (C.A.G.).

REFERENCES

1. **O'Sullivan BP, Freedman SD.** 2009. Cystic fibrosis. Lancet **373:**1891–1904. http://dx.doi.org/10.1016/S0140-6736(09)60327-5.
2. **Rowe SM, Miller S, Sorscher EJ.** 2005. Cystic fibrosis. N. Engl. J. Med. **352:**1992–2001. http://dx.doi.org/10.1056/NEJMra043184.
3. **Delhaes L, Monchy S, Frealle E, Hubans C, Salleron J, Leroy S, Prevotat A, Wallet F, Wallaert B, Dei-Cas E, Sime-Ngando T, Chabe M, Viscogliosi E.** 2012. The airway microbiota in cystic fibrosis: a complex fungal and bacterial community—implications for therapeutic management. PLoS One **7:**e36313. http://dx.doi.org/10.1371/journal.pone.0036313.
4. **Lynch SV, Bruce KD.** 2013. The cystic fibrosis airway microbiome. Cold Spring Harb. Perspect. Med. **3:**a009738. http://dx.doi.org/10.1101/cshperspect.a009738.
5. **Shoseyov D, Brownlee KG, Conway SP, Kerem E.** 2006. Aspergillus bronchitis in cystic fibrosis. Chest **130:**222–226. http://dx.doi.org/10.1378/chest.130.1.222.
6. **Amin R, Dupuis A, Aaron SD, Ratjen F.** 2010. The effect of chronic infection with Aspergillus fumigatus on lung function and hospitalization in patients with cystic fibrosis. Chest **137:**171–176. http://dx.doi.org/10.1378/chest.09-1103.
7. **Leclair LW, Hogan DA.** 2010. Mixed bacterial-fungal infections in the CF respiratory tract. Med. Mycol. **48**(Suppl 1)**:**S125–S132. http://dx.doi.org/10.3109/13693786.2010.521522.
8. **Phelan VV, Liu WT, Pogliano K, Dorrestein PC.** 2012. Microbial metabolic exchange—the chemotype-to-phenotype link. Nat. Chem. Biol. **8:**26–35. http://dx.doi.org/10.1038/nchembio.739.
9. **Davies J.** 2013. Specialized microbial metabolites: functions and origins. J. Antibiot. (Tokyo) **66:**361–364. http://dx.doi.org/10.1038/ja.2013.61.
10. **Mowat E, Rajendran R, Williams C, McCulloch E, Jones B, Lang S, Ramage G.** 2010. Pseudomonas aeruginosa and their small diffusible extracellular molecules inhibit Aspergillus fumigatus biofilm formation. FEMS Microbiol. Lett. **313:**96–102. http://dx.doi.org/10.1111/j.1574-6968.2010.02130.x.
11. **Moree WJ, Phelan VV, Wu CH, Bandeira N, Cornett DS, Duggan BM, Dorrestein PC.** 2012. Interkingdom metabolic transformations captured by microbial imaging mass spectrometry. Proc. Natl. Acad. Sci. U. S. A. **109:**13811–13816. http://dx.doi.org/10.1073/pnas.1206855109.
12. **Price-Whelan A, Dietrich LE, Newman DK.** 2006. Rethinking 'secondary' metabolism: physiological roles for phenazine antibiotics. Nat. Chem. Biol. **2:**71–78. http://dx.doi.org/10.1038/nchembio764.
13. **Pierson LS, III, Pierson EA.** 2010. Metabolism and function of phenazines in bacteria: impacts on the behavior of bacteria in the environment and biotechnological processes. Appl. Microbiol. Biotechnol. **86:**1659–1670. http://dx.doi.org/10.1007/s00253-010-2509-3.
14. **Mentel M, Ahuja EG, Mavrodi DV, Breinbauer R, Thomashow LS, Blankenfeldt W.** 2009. Of two make one: the biosynthesis of phenazines. Chembiochem **10:**2295–2304. http://dx.doi.org/10.1002/cbic.200900323.
15. **Blankenfeldt W, Kuzin AP, Skarina T, Korniyenko Y, Tong L, Bayer P,**

Janning P, Thomashow LS, Mavrodi DV. 2004. Structure and function of the phenazine biosynthetic protein PhzF from Pseudomonas fluorescens. Proc. Natl. Acad. Sci. U. S. A. **101:**16431–16436. http://dx.doi.org/10.1073/pnas.0407371101.

16. **Parsons JF, Song FH, Parsons L, Calabrese K, Eisenstein E, Ladner JE.** 2004. Structure and function of the phenazine biosynthesis protein PhzF from Pseudomonas fluorescens 2-79. Biochemistry **43:**12427–12435. http://dx.doi.org/10.1021/bi049059z.
17. **Ahuja EG, Janning P, Mentel M, Graebsch A, Breinbauer R, Hiller W, Costisella B, Thomashow LS, Mavrodi DV, Blankenfeldt W.** 2008. PhzA/B catalyzes the formation of the tricycle in phenazine biosynthesis. J. Am. Chem. Soc. **130:**17053–17061. http://dx.doi.org/10.1021/ja806325k.
18. **Mavrodi DV, Bonsall RF, Delaney SM, Soule MJ, Phillips G, Thomashow LS.** 2001. Functional analysis of genes for biosynthesis of pyocyanin and phenazine-1-carboxamide from Pseudomonas aeruginosa PAO1. J. Bacteriol. **183:**6454–6465. http://dx.doi.org/10.1128/JB.183.21.6454-6465.2001.
19. **Recinos DA, Sekedat MD, Hernandez A, Cohen TS, Sakhtah H, Prince AS, Price-Whelan A, Dietrich LE.** 2012. Redundant phenazine operons in Pseudomonas aeruginosa exhibit environment-dependent expression and differential roles in pathogenicity. Proc. Natl. Acad. Sci. U. S. A. **109:**19420–19425. http://dx.doi.org/10.1073/pnas.1213901109.
20. **Jacobs MA, Alwood A, Thaipisuttikul I, Spencer D, Haugen E, Ernst S, Will O, Kaul R, Raymond C, Levy R, Chun-Rong L, Guenthner D, Bovee D, Olson MV, Manoil C.** 2003. Comprehensive transposon mutant library of Pseudomonas aeruginosa. Proc. Natl. Acad. Sci. U. S. A. **100:**14339–14344. http://dx.doi.org/10.1073/pnas.2036282100.
21. **Qiu D, Damron FH, Mima T, Schweizer HP, Yu HD.** 2008. PBAD-based shuttle vectors for functional analysis of toxic and highly regulated genes in Pseudomonas and Burkholderia spp. and other bacteria. Appl. Environ. Microbiol. **74:**7422–7426. http://dx.doi.org/10.1128/AEM.01369-08.
22. **Liu WT, Yang YL, Xu Y, Lamsa A, Haste NM, Yang JY, Ng J, Gonzalez D, Ellermeier CD, Straight PD, Pevzner PA, Pogliano J, Nizet V, Pogliano K, Dorrestein PC.** 2010. Imaging mass spectrometry of intraspecies metabolic exchange revealed the cannibalistic factors of Bacillus subtilis. Proc. Natl. Acad. Sci. U. S. A. **107:**16286–16290. http://dx.doi.org/10.1073/pnas.1008368107.
23. **Booth BL, Haszeldine RN, Laali K.** 1980. Alkyltrifluoromethanesulphonates as alkylating reagents for aromatic compounds. J. Chem. Soc. Perkin 1 **12:**2887–2893.
24. **Yang JY, Phelan VV, Simkovsky R, Watrous JD, Trial RM, Fleming TC, Wenter R, Moore BS, Golden SS, Pogliano K, Dorrestein PC.** 2012. Primer on agar-based microbial imaging mass spectrometry. J. Bacteriol. **194:**6023–6028. http://dx.doi.org/10.1128/JB.00823-12.
25. **Yang YL, Xu Y, Kersten RD, Liu WT, Meehan MJ, Moore BS, Bandeira N, Dorrestein PC.** 2011. Connecting chemotypes and phenotypes of cultured marine microbial assemblages by imaging mass spectrometry. Angew. Chem. Int. Ed. Engl. **50:**5839–5842. http://dx.doi.org/10.1002/anie.201101225.
26. **Yang YL, Xu Y, Straight P, Dorrestein PC.** 2009. Translating metabolic exchange with imaging mass spectrometry. Nat. Chem. Biol. **5:**885–887. http://dx.doi.org/10.1038/nchembio.252.
27. **Boukhalfa H, Crumbliss AL.** 2002. Chemical aspects of siderophore mediated iron transport. Biometals **15:**325–339. http://dx.doi.org/10.1023/A:1020218608266.
28. **Visca P, Imperi F, Lamont IL.** 2007. Pyoverdine siderophores: from biogenesis to biosignificance. Trends Microbiol. **15:**22–30. http://dx.doi.org/10.1016/j.tim.2006.11.004.
29. **Cornelis P.** 2010. Iron uptake and metabolism in pseudomonads. Appl. Microbiol. Biotechnol. **86:**1637–1645. http://dx.doi.org/10.1007/s00253-010-2550-2.
30. **Schrettl M, Bignell E, Kragl C, Joechl C, Rogers T, Arst HN, Jr, Haynes K, Haas H.** 2004. Siderophore biosynthesis but not reductive iron assimilation is essential for *Aspergillus fumigatus* virulence. J. Exp. Med. **200:**1213–1219. http://dx.doi.org/10.1084/jem.20041242.
31. **Poole K, McKay GA.** 2003. Iron acquisition and its control in Pseudomonas aeruginosa: many roads lead to Rome. Front. Biosci. **8:**d661–d686. http://dx.doi.org/10.2741/1051.
32. **Haas H.** 2003. Molecular genetics of fungal siderophore biosynthesis and uptake: the role of siderophores in iron uptake and storage. Appl. Microbiol. Biotechnol. **62:**316–330. http://dx.doi.org/10.1007/s00253-003-1335-2.
33. **Dietrich LE, Price-Whelan A, Petersen A, Whiteley M, Newman DK.** 2006. The phenazine pyocyanin is a terminal signalling factor in the quorum sensing network of Pseudomonas aeruginosa. Mol. Microbiol. **61:**1308–1321. http://dx.doi.org/10.1111/j.1365-2958.2006.05306.x.
34. **Jimenez PN, Koch G, Thompson JA, Xavier KB, Cool RH, Quax WJ.** 2012. The multiple signaling systems regulating virulence in Pseudomonas aeruginosa. Microbiol. Mol. Biol. Rev. **76:**46–65. http://dx.doi.org/10.1128/MMBR.05007-11.
35. **Passador L, Cook JM, Gambello MJ, Rust L, Iglewski BH.** 1993. Expression of Pseudomonas aeruginosa virulence genes requires cell-to-cell communication. Science **260:**1127–1130. http://dx.doi.org/10.1126/science.8493556.
36. **Hogan DA, Vik A, Kolter R.** 2004. A Pseudomonas aeruginosa quorum-sensing molecule influences Candida albicans morphology. Mol. Microbiol. **54:**1212–1223. http://dx.doi.org/10.1111/j.1365-2958.2004.04349.x.
37. **Pearson JP, Passador L, Iglewski BH, Greenberg EP.** 1995. A second N-acylhomoserine lactone signal produced by Pseudomonas aeruginosa. Proc. Natl. Acad. Sci. U. S. A. **92:**1490–1494. http://dx.doi.org/10.1073/pnas.92.5.1490.
38. **McGrath S, Wade DS, Pesci EC.** 2004. Dueling quorum sensing systems in Pseudomonas aeruginosa control the production of the Pseudomonas quinolone signal (PQS). FEMS Microbiol. Lett. **230:**27–34. http://dx.doi.org/10.1016/S0378-1097(03)00849-8.
39. **Déziel E, Lepine F, Milot S, He JX, Mindrinos MN, Tompkins RG, Rahme LG.** 2004. Analysis of Pseudomonas aeruginosa 4-hydroxy-2-alkylquinolines (HAQs) reveals a role for 4-hydroxy-2-heptylquinoline in cell-to-cell communication. Proc. Natl. Acad. Sci. U. S. A. **101:**1339–1344. http://dx.doi.org/10.1073/pnas.0307694100.
40. **Diggle SP, Matthijs S, Wright VJ, Fletcher MP, Chhabra SR, Lamont IL, Kong XL, Hider RC, Cornelis P, Camara M, Williams P.** 2007. The Pseudomonas aeruginosa 4-quinolone signal molecules HHQ and PQS play multifunctional roles in quorum sensing and iron entrapment. Chem. Biol. **14:**87–96. http://dx.doi.org/10.1016/j.chembiol.2006.11.014.
41. **Dubern JF, Diggle SP.** 2008. Quorum sensing by 2-alkyl-4-quinolones in Pseudomonas aeruginosa and other bacterial species. Mol. Biosyst. **4:**882–888. http://dx.doi.org/10.1039/b803796p.
42. **Heeb S, Fletcher MP, Chhabra SR, Diggle SP, Williams P, Camara M.** 2011. Quinolones: from antibiotics to autoinducers. FEMS Microbiol. Rev. **35:**247–274. http://dx.doi.org/10.1111/j.1574-6976.2010.00247.x.
43. **Huse H, Whiteley M.** 2011. 4-Quinolones: smart phones of the microbial world. Chem. Rev. **111:**152–159. http://dx.doi.org/10.1021/cr100063u.
44. **Ochsner UA, Reiser J.** 1995. Autoinducer-mediated regulation of rhamnolipid biosurfactant synthesis in Pseudomonas aeruginosa. Proc. Natl. Acad. Sci. U. S. A. **92:**6424–6428. http://dx.doi.org/10.1073/pnas.92.14.6424.
45. **Soberón-Chávez G, Lepine F, Deziel E.** 2005. Production of rhamnolipids by Pseudomonas aeruginosa. Appl. Microbiol. Biotechnol. **68:**718–725. http://dx.doi.org/10.1007/s00253-005-0150-3.
46. **Dietrich LE, Teal TK, Price-Whelan A, Newman DK.** 2008. Redox-active antibiotics control gene expression and community behavior in divergent bacteria. Science **321:**1203–1206. http://dx.doi.org/10.1126/science.1160619.
47. **Ramos I, Dietrich LE, Price-Whelan A, Newman DK.** 2010. Phenazines affect biofilm formation by Pseudomonas aeruginosa in similar ways at various scales. Res. Microbiol. **161:**187–191. http://dx.doi.org/10.1016/j.resmic.2010.01.003.
48. **Hernandez ME, Kappler A, Newman DK.** 2004. Phenazines and other redox-active antibiotics promote microbial mineral reduction. Appl. Environ. Microbiol. **70:**921–928. http://dx.doi.org/10.1128/AEM.70.2.921-928.2004.
49. **Wang Y, Kern SE, Newman DK.** 2010. Endogenous phenazine antibiotics promote anaerobic survival of Pseudomonas aeruginosa via extracellular electron transfer. J. Bacteriol. **192:**365–369. http://dx.doi.org/10.1128/JB.01188-09.
50. **Wang Y, Newman DK.** 2008. Redox reactions of phenazine antibiotics with ferric (hydr)oxides and molecular oxygen. Environ. Sci. Technol. **42:**2380–2386. http://dx.doi.org/10.1021/es702290a.
51. **Wang Y, Wilks JC, Danhorn T, Ramos I, Croal L, Newman DK.** 2011. Phenazine-1-carboxylic acid promotes bacterial biofilm development via ferrous iron acquisition. J. Bacteriol. **193:**3606–3617. http://dx.doi.org/10.1128/JB.00396-11.

52. **Imperi F, Tiburzi F, Visca P.** 2009. Molecular basis of pyoverdine siderophore recycling in Pseudomonas aeruginosa. Proc. Natl. Acad. Sci. U. S. A. **106:**20440–20445. http://dx.doi.org/10.1073/pnas.0908760106.
53. **Okegbe C, Sakhtah H, Sekedat MD, Price-Whelan A, Dietrich LE.** 2012. Redox eustress: roles for redox-active metabolites in bacterial signaling and behavior. Antioxid. Redox Signal. **16:**658–667. http://dx.doi.org/10.1089/ars.2011.4249.
54. **Blainey PC, Milla CE, Cornfield DN, Quake SR.** 2012. Quantitative analysis of the human airway microbial ecology reveals a pervasive signature for cystic fibrosis. Sci. Transl. Med. **4:**153ra30. http://dx.doi.org/10.1126/scitranslmed.3004458.
55. **Hunter RC, Klepac-Ceraj V, Lorenzi MM, Grotzinger H, Martin TR, Newman DK.** 2012. Phenazine content in the cystic fibrosis respiratory tract negatively correlates with lung function and microbial complexity. Am. J. Respir. Cell Mol. Biol. **47:**738–745. http://dx.doi.org/10.1165/rcmb.2012-0088OC.